

DYNAMICS OF DUNES
IN AN INTERTIDAL ENVIRONMENT
AT NAUSET INLET, MASSACHUSETTS

by

GERALD MATISOFF

Submitted in Partial Fulfillment
of the Requirements for the
Degree of Bachelor of Science
at the
MASSACHUSETTS INSTITUTE OF TECHNOLOGY
June, 1973

Signature of Author.....
Department of Earth and Planetary Sciences, 21 May, 1973

Certified by.....
Thesis Supervisor

Accepted by.....
Chairman, Departmental Committee on Theses

WITHDRAWN
FROM
MIT LIBRARIES

ABSTRACT

The dynamics of bedforms in an intertidal environment are fundamentally a function of the nature of the tidal flow. Some aspects of tidal flow may be characterized by methods previously applied to unidirectional, open channel flow, while other aspects are peculiar to the tidal environment. Any attempt to study the changes in the dynamics of bedforms throughout a tidal cycle must account for both of these aspects. Previous investigators have either failed to study the entire problem, or have used methods and drawn conclusions which are not entirely justified. Thus, an apparatus which will allow for all of the necessary data is presented.

Equilibrium bedform configurations have been shown to be functions of depth, velocity and particle size (Southard, 1971). Proposed extensions of the bedform boundaries have been drawn to allow for greater depths occurring in field conditions. Due to the absence of any data to date, a semi-quantitative, theoretical prediction of how depth and velocity vary as a function of time in the tidal cycle is presented and superimposed on the bed stability diagram, yielding excellent agreement with the observed features.

By previous field investigations and aerial reconnaissance, Nauset Inlet was chosen as the study area. Several photographs of outstanding examples of bed features at Nauset Inlet and other possible study areas are included.

TABLE OF CONTENTS

	<u>Page Number</u>
Abstract.....	1
Table of Contents.....	2
List of Figures.....	3
Acknowledgements.....	4
Background and General Nature of the Problem.....	5
Selection and Nature of the Study Area.....	15
Methods.....	26
References.....	31
Appendix 1: Sieve Analyses.....	33
Appendix 2: Photographs of Bed Features in Other Possible Study Areas.....	35
Appendix 3: Derivation of Mean Velocity from Known Surface Velocity.....	43

LIST OF FIGURES

<u>Figure Number</u>	<u>Title</u>	<u>Page Number</u>
1.....	Depth and Velocity as a Function of Time in a Tidal Cycle.....	8
2.....	Time Pathline on Bed Stability Fields..	12
3.....	Index Photograph of Study Area.....	16

<u>Photo Number</u>	<u>Title</u>	<u>Page Number</u>
1.....	Nauset Inlet Basin.....	18
2.....	Study Location.....	19
3.....	Fully Developed Dunes.....	20
4.....	Planed Linear Dunes.....	21
5.....	Transition from Ripples to Dunes.	22
6.....	Orthogonal Interference Pattern..	23
7.....	Ebb Shield.....	24
8.....	Erosion Scarp.....	25
4.....	Plan View of Apparatus.....	28
5.....	Sieve Analysis, Linear Dunes.....	33
6.....	Sieve Analysis, Fully Developed Dunes..	34

Appendix 2: Photographs of Other Areas

1.....	Intertidal Sand Bar.....	36
2.....	Duned Channel Bottom.....	37
3.....	Dunes on a Sand Bar.....	38
4.....	Sand Ridges.....	39
5.....	Sand Waves.....	40
6.....	Sand Waves.....	41
7.....	Interference Sand Waves.....	42

ACKNOWLEDGEMENTS

I gratefully acknowledge thanks to all those who offered assistance and guidance to me and helped make this thesis possible: to Professor Brian R. Pearce and Professor Donald R. F. Harleman of the Department of Civil Engineering, and to Professor Erik L. Mollo-Christensen of the Department of Meteorology, for their helpful suggestions; to Professor Ole S. Madsen of the Department of Civil Engineering for his limitless patience and guidance in explaining dynamic problems; and above all, to Professor John B. Southard of the Department of Earth and Planetary Sciences, who was a constant source of inspiration and encouragement, and so generously offered his facilities.

BACKGROUND AND GENERAL
NATURE OF THE PROBLEM

Observations and study of bed configurations in alluvial channels have been well documented. The same cannot be said for tidal environments, primarily because investigators are troubled by the nature of tidal flow. The difference between river and tidal flow lies solely in the character of the flow, but even though tidal currents are undergoing continuous changes, they run for a period of time within specific flow regimes, corresponding to conditions of unidirectional flow and producing bed configurations. Considerable effort has been expended by many investigators to determine the equilibrium bedform as a function, among other things, of depth, velocity, and particle size. Guy, Simons, and Richardson (1966) summarize five years of such a study.

Laboratory studies of bed configurations are generally restricted to depths less than 0.5 m and widths less than 2.5 m due to physical limitations of equipment. In the tidal environments considered as possible study locations for this project, there is a range of depths from 0 - 3 m; and during periods of the tidal cycle, the flow conditions are such that the flow may be characterized as infinitely wide, open channel flow, while during other periods of the tidal cycle, there is no flow at all. Thus, alluvial channel conditions may be considered steady, while tidal conditions are dynamic.

Exactly how these dynamic conditions affect the bottom geometry in intertidal environments is not well understood. Boothroyd

(1969) and Hartwell (1969) qualitatively discuss the effects of the bimonthly spring to neap tidal cycle on the migration rates and general geometry of the bedforms, noting that not only do the bedforms respond to changing tidal conditions, but zones of flood and ebb dominance on intertidal sand bodies also change. They do not, however, discuss how the dynamic changes of tidal flow during a tidal cycle affect the bed configurations. Klein (1970) and Klein and Whaley (1972) attempt this problem, claiming significant results. However, one may seriously question the method of investigation of Klein and Whaley, and since the method of investigation is vital for an accurate solution of the problem, further discussion of this matter is contained in the later chapter on methods.

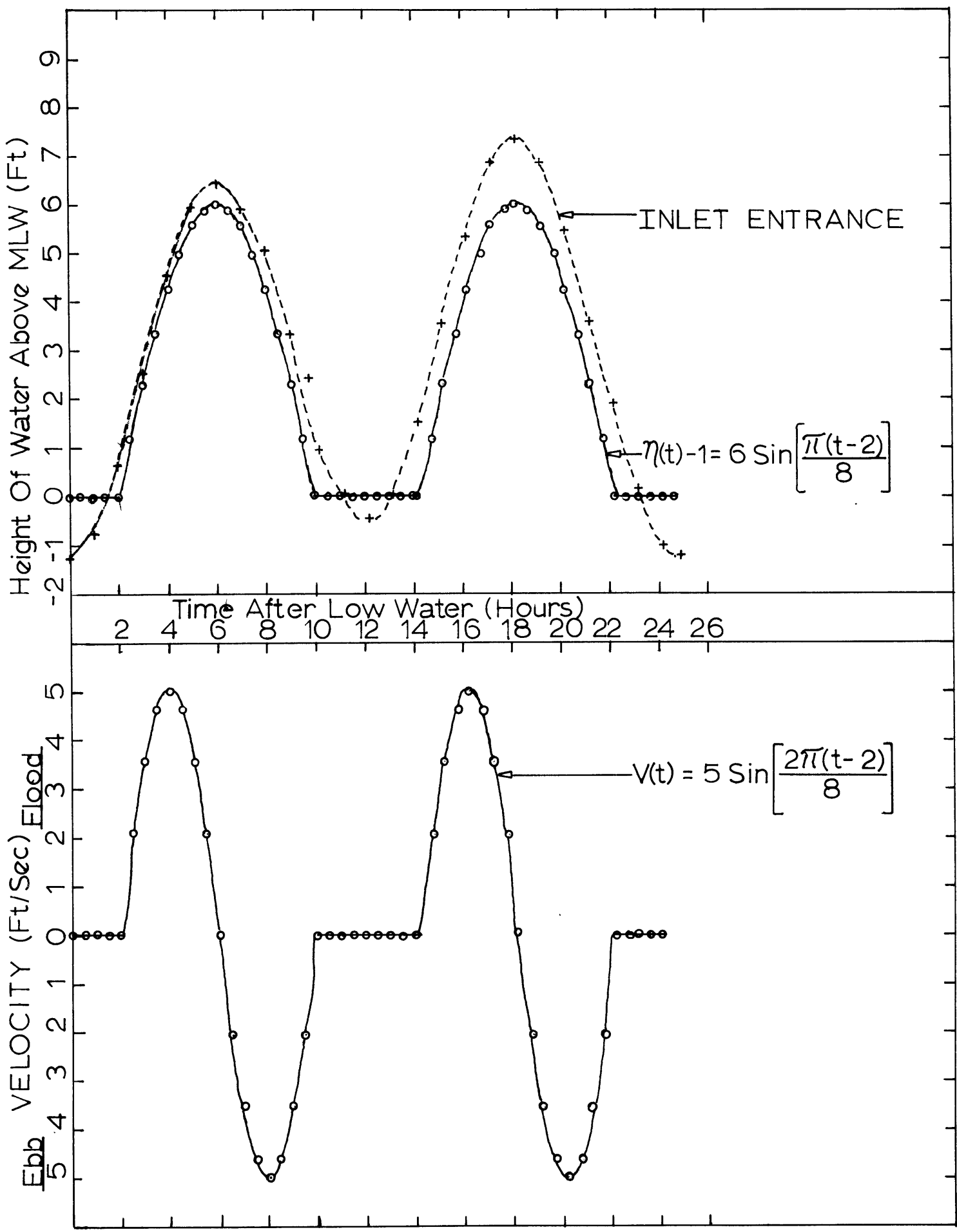
Another factor on which equilibrium conditions depend and may be controlled in laboratory experiments but not in field studies is the particle size. Most natural sands approximate a Gaussian distribution of grain sizes, and in some laboratory experiments the sands are sieved so that only one small segment of the distribution is used. Characterizations of the equilibrium bedforms as functions of depth, velocity, and grain size (Southard, 1971) have not attempted to define the relative effects of sorting. The distribution of grain sizes in field environments may then introduce effects not accounted for in such a bed stability diagram. Bruun (1960) notes that graded sands seem to have slightly less total bed friction than uniform sands. However, sieve analyses of sand from two locations of the study area (see Appendix 1) show that by the

classification introduced by Folk (1965) the sands are moderately to very well sorted, implying that the effects of the grain size distribution will be minimal. Since the median grain size of the two sands is about .4 mm, the .45 mm bed stability field derived by Southard will be used. Comparison of the observed bedform as a function of depth and velocity will be made with proposed extensions of the equilibrium bedform lines in his diagram. Since, however, no data have yet been collected, a general procedure of this comparison and a method for estimating depth and velocity in an intertidal environment are contained in the discussion which follows.

For a spring tide, the surface elevation, η , of the water level at the entrance to Nauset Inlet can be seen in tide tables to vary from about 7 feet to -1 foot relative to the mean low tide level. Thus the amplitude of the tidal reach is about 4 feet. The proposed area of study, however, is landward of the location of measurement. Hence, it is at a higher elevation, and is submerged by less water for a shorter period of time than the entrance to the inlet. The study area is approximately 1 foot higher than the mean low tide level. Based on tidal elevation predictions for the inlet entrance, this means that the 'effective' tidal cycle is only about 8 hours. This is illustrated in the top half of figure 1, where the dashed curve crosses the 1-foot elevation level at 2 hours after low tide, and again about 8 hours later.

Determination of the exact nature of the variation of the depth at the study location is a difficult problem to predict.

Figure 1



Keulegažn, 1967, presents a method based on continuity principles relating the elevation outside the inlet to the mean elevation inside. Required in his method are a variety of geometrical properties of the inlet basin, and an attempt to solve the problem by his approach would require several assumptions: (1) that the area of shoals in the basin is small compared to the total area of the basin, (2) that water entering the basin is instantaneously assumed to be diffused throughout the basin--yielding the absurd conclusion, and (3) that the velocity everywhere in the basin at all times is equal to zero.

In lieu of the geometry of this particular inlet, and the fact that the study location is along a bank of a secondary tidal channel--where the velocities are certainly not equal to zero, and where continuity above and around shoals would be difficult to apply--the author feels that a solution by Keulegan's approach would not only be tedious, but probably unprofitable in that it would yield a highly dubious result. Therefore, a solution by this approach has been rejected. Application of his method to this particular problem is, however, the only method of an 'exact' solution of the problem. Therefore, since depth and velocity are to be measured in the field right at the study area, generating the true solution directly, no exact solution is necessary; only an approximate solution is needed to yield the general nature of the depth and velocity curves.

Solution by Keulegan's method would yield this approximate solution, but a much simpler and perhaps as accurate a method is

suggested. Assuming that as the study location becomes submerged, it assumes a sinusoidal variation of depth with a period of 8 hours and a mean amplitude of approximately 3 feet, there for the one or two spring tidal cycles under consideration, the height of the water above the mean low water level, η , may be approximated as

$$\eta(t) = 1 + 6 \sin \left[\frac{\pi(t-2)}{8} \right], \quad 2 \leq t \leq 10$$

where t is the time in hours after low water at the entrance to the inlet. For all other values of $t \leq 12.5$, $\eta = 1$. The height of the water above the study area at time t is, then, by definition, equal to $\eta - 1$.

It is to be remembered that this is only an approximation, and is based on a uniform 8 hour tidal cycle at the sample location. But for the purposes of approximating the depth variation on Southard's bed stability diagram, it should be quite adequate. This curve is shown by the solid line in the top half of figure 1.

The velocity variation may be approximated in the same manner. Here it is assumed that at high and low water the velocity at the study area is equal to zero, and varies sinusoidally between slack-water periods. Hence, the velocity is zero every 4 hours when water is above the study area, and obviously zero when there is no water. Assuming also that the mean maximum velocity is 5 ft/sec then a velocity curve may be derived:

$$v(t) = 5 \sin \left[\frac{2\pi(t-2)}{8.0} \right], \quad 2 \leq t \leq 10,$$

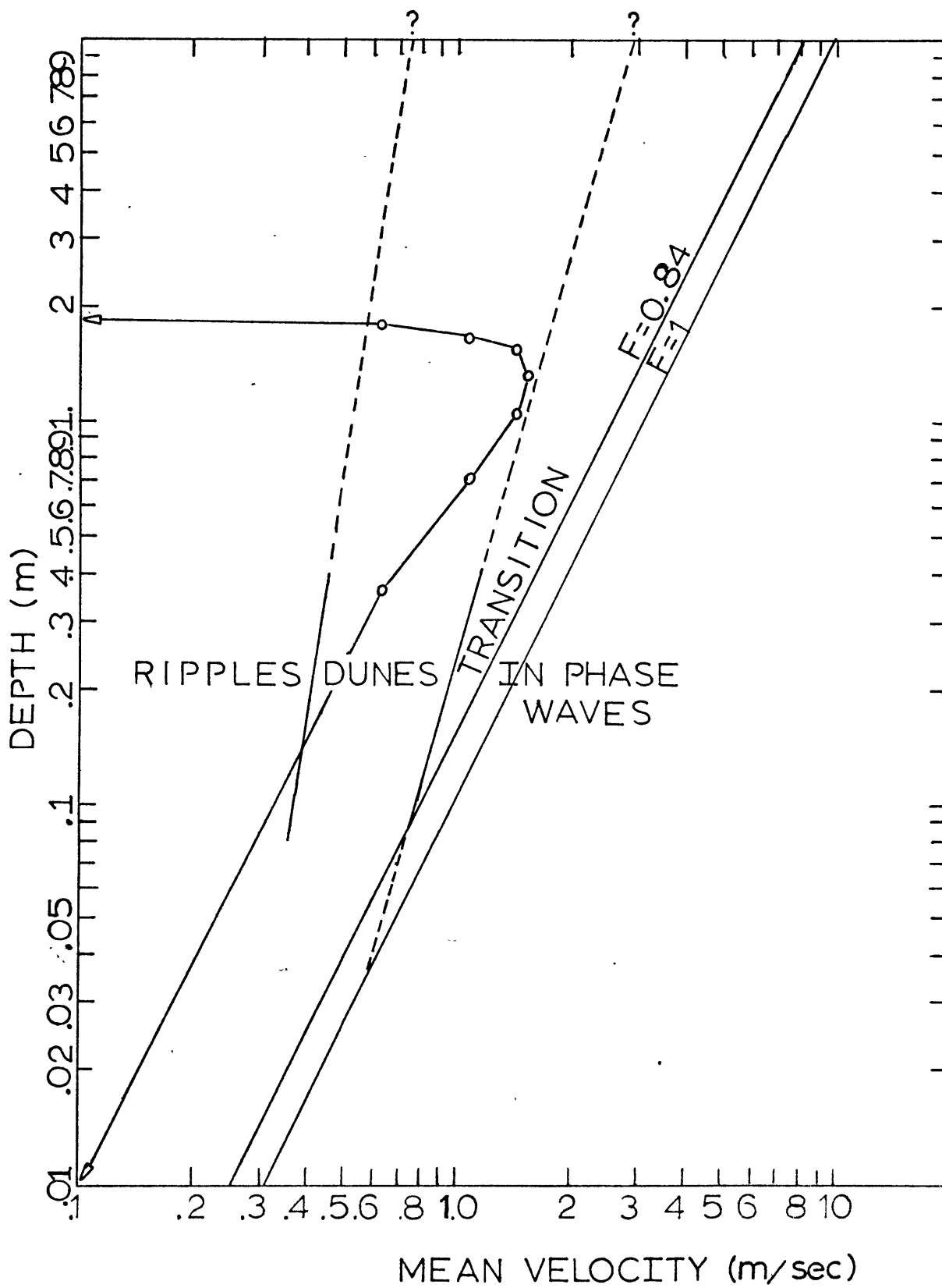
where t is the time in hours after low water at the entrance to

the inlet. For all other values of $t < 12.5$, $V = 0$. This velocity is taken to be the mean velocity over the depth as discussed in detail in Appendix 3 .

It is to be emphasized that these relations are not absolute predictions of how velocity and depth will vary at the study area over a tidal cycle--such predictions are impossible without further data--but rather a plausible representation of what might be found when the actual measurements are taken. That is, upon acquisition of the data, curves of this nature may be drawn to precisely define a general time pathline in the bed stability diagram. Since measurements will not be taken until at least .3 m (1 ft) of water covers the study area (to avoid transient effects and extreme unsteady flow) a precise prediction of the depth is not absolutely necessary because of the general nature of the diagram and a logarithmic depth scale.

Figure 2 is thus a representation of a possible time pathline over the bed stability fields for the hydrodynamic conditions present at the study location. The time pathline of velocity and depth is represented by the curved line in the ripple and dune fields. The interval between any two of the points defining this time pathline is one-half hour. Taking the starting point of the curve to be when flooding of the study area begins, then the beginning of the pathline is in the lower-left corner of the graph. The first half hour is spent predominantly in the ripple field, although at very low depths. Upon entering the range of depths which are measurable, and hence under consideration, the pathline spends the

FIGURE 2



next 3 hours in the dune regime--certainly long enough to establish some well-developed dunes. Also, for the majority of this time period the water depths exceed two feet. The next half hour (that adjacent to slack high water) is spent at very low velocities in the ripple, no migration, and no movement regimes. When ebbing starts, the path is reversed, as previously hypothesized by Bruun (1960). These observations help explain why dunes, and sometimes ripples superimposed on dunes, are observed at the study area. Even if the original estimate of the mean maximum velocity was incorrect by being too large by one or two feet per second, this effect would still take place predominantly in the dune field.

In a natural environment, an asymmetry exists in both the depth and velocity time profiles, as previously discussed in the section pertaining to dynamic environments. This would result in bedforms in some areas remaining metastably oriented in the flood or ebb direction--whichever had the strongest flow conditions during the previous tidal cycles. The resulting effect on the time path-line in the bed stability diagram would not be a retraced curve as noted for the symmetrical case, but a hysteresis loop; perhaps containing discontinuities in the dune regime, where formation and migration of bedforms during the weaker phase does not take place. In some cases this weaker phase results in only 'planing off the tops' of the oppositely oriented bedforms; decreasing their amplitudes, and infilling their scour holes; and creating more sinuous bedforms. Other times, lower order bedforms will be superimposed on higher order bedforms of the opposite orientation. These effects

have been observed in the field by the author, and have been recorded by Klein (1970) and Boothroyd (1969).

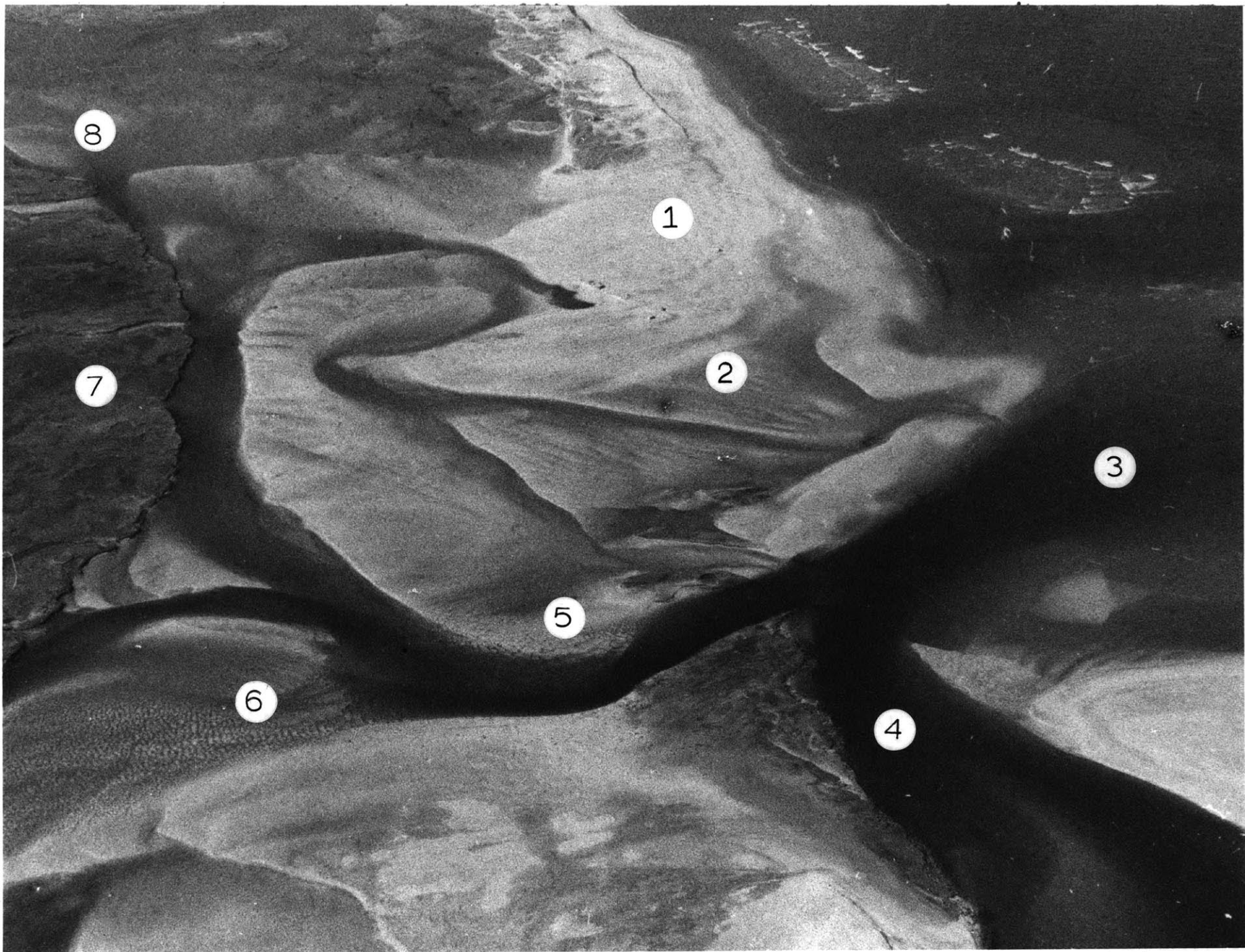
It is to be noted that the amplitude of dunes has been reported (Allen, 1970; Yalin, 1964; and other authors) to be partially a function of the depth of the water. Hence, much larger dunes may be observed in the field than in laboratory studies. This relationship of dunes with depth of flow is not well understood, since comparison of both experimental and field data with the results proposed by these two authors yield very poor agreement. Therefore, no attempt will be made (now or after collection of the data) to make theoretical predictions of the geometrical properties of the dunes. Also, if predictions of amplitude with depth are in poor agreement for a constant depth, evaluation of the problem for a sinusoidally varying depth would be even more complex and yield much greater scatter of the data.

Thus, until the actual acquisition of data is obtained, bedforms in intertidal environments may be treated in a manner similar to those in alluvial channels, differing only in the nature of their flow, and yielding excellent agreement with the depth-velocity-particle size bed stability diagram.

SELECTION AND NATURE OF THE STUDY AREA

Dunes have been observed by John Southard in the intertidal environments of Nauset Inlet, Eastham, Massachusetts and the tidal channel off First Encounter Beach, Orleans, Massachusetts. In addition, Nauset Inlet has displayed a highly dynamic character and exhibits a variety of bed configurations within short distances of each other. For this reason, preliminary plans for construction of the equipment were based on the assumption that Nauset Inlet was to be the study area. Since the nearest parking lot yielding access to the inlet by land at low tide is about $2\frac{1}{2}$ miles from the inlet itself, the equipment was designed to be as simple and lightweight as possible. This of course puts restrictions on the strength of materials which may be used, and thus somewhat limits the conditions in which the apparatus may be operated. Therefore, before final equipment construction was undertaken, an aerial reconnaissance of these and other possible study areas was done, determining the distribution of bedforms within each area, and their accessibility by automobile. After completion of the reconnaissance and study of the aerial photographs, Nauset Inlet was still selected as the major study area, although First Encounter Beach may be used to test the equipment.

This section contains a collection of photographs of the study area. Particular area of interest, including the actual spot selected for study, pictures of the bedforms, and a view of the entire inlet region itself are shown. In addition, a collection of



photographs of outstanding examples of bed features, which were observed to exist in other areas not selected for study, may be found in Appendix 2.

On the page opposite is an enlarged aerial photograph of the Nauset Inlet study area. Specific features, some of which may be seen in the figures, have been assigned numbers; the index is listed below:

- ① Erosion scarp. Figure 8 following.
- ② Planed linear dunes. Figure 4 following.
- ③ Nauset Inlet.
- ④ Primary tidal channel.
- ⑤ Actual study location. Figure 2 following.
- ⑥ Dune field. Figure 2 following.
- ⑦ Marshland.
- ⑧ Orthogonal interference pattern. Figure 6 following.

Not shown:

- Figure 1 Nauset Inlet Basin.
- Figure 3 Fully developed dunes.
- Figure 5 Transition from ripples to dunes.
- Figure 7 Ebb shield.



Figure 1. Aerial photograph of Nauset Inlet and much of the tidal basin at low tide. Note formation of two flood tidal deltas divided by a secondary tidal channel. Study area located beside this secondary tidal channel. Primary tidal channel evident in left side of photograph, clearly showing containment of most of the water within the channel network. Turbidity to the seaward side of the inlet is slightly visible. Note also formation of an ebb-tidal delta off the southern side of the inlet. Geometry of the inlet suggests that the direction of littoral drift and inlet migration is diagonally from right to left, in agreement with previous observations (Strahler, 1966).



Figure 2. Aerial photo pinpointing exact location of proposed study. Note formation of well-developed dunes with spacing ~ 5 feet and amplitudes ~ $1\frac{1}{2}$ feet. Across secondary tidal channel (too deep and too wide to attempt crossing without a boat) is development of dune field, quite visible from study location. To the right of study area are three or four remnants of marshland, indicating infilling and migration of flood-tidal delta.



Figure 3. Well-developed dunes as observed on the ground during low water. Note irregular nature of dunes, and superimposed ripples. The ripples show extreme variability in their orientations implying that they developed during late stage, shallow water conditions, and their dynamics were controlled by local changes in slope and drainage. Photo courtesy of John Southard.



Figure 4. Planed, flood-oriented, linear dunes as observed in the field during low water. Note high degree of regularity of the planed-off crests. These dunes developed in a slightly lower flow regime than those in Figure 3, and hence, a high degree of regularity exists. The weaker ebb phase did not destroy the pre-existing dunes, but managed to plane the crests. Note also the superimposed ripples controlled by late-stage activity as discussed in figure 3. Photo courtesy of John Southard.



Figure 5. Transition from ripples to dunes as observed in the field during low water. This bed configuration developed under slightly lower flow regime conditions than the dunes in figure 4, but in a higher flow regime than necessary for just ripples. Photo courtesy of John Southard.



Figure 6. Aerial photograph of an orthogonal interference pattern in a sand body probably the result of intersecting sets of ripples and dunes formed by an elliptical circulation of flood and ebb waters. Character of sand body resembles that of an alluvial delta, and since sand body is building sandward of the inlet (see reference photo at beginning of this section), the features at the right are probably flood controlled.



Figure 7. Aerial photograph of an ebb shield off the lower left corner of the reference photo. Note formation of what appear to be sand waves and linear dunes along the left side of the shield. This area is not visible from main study area and is accessible only by boat. Photo taken at low tide.



Figure 8. Aerial photograph of the portion of Nauset Beach adjacent to the inlet region. Note different levels of erosional surfaces. Linear dune field present in upper central section of photo. Photo taken at low tide.

METHODS

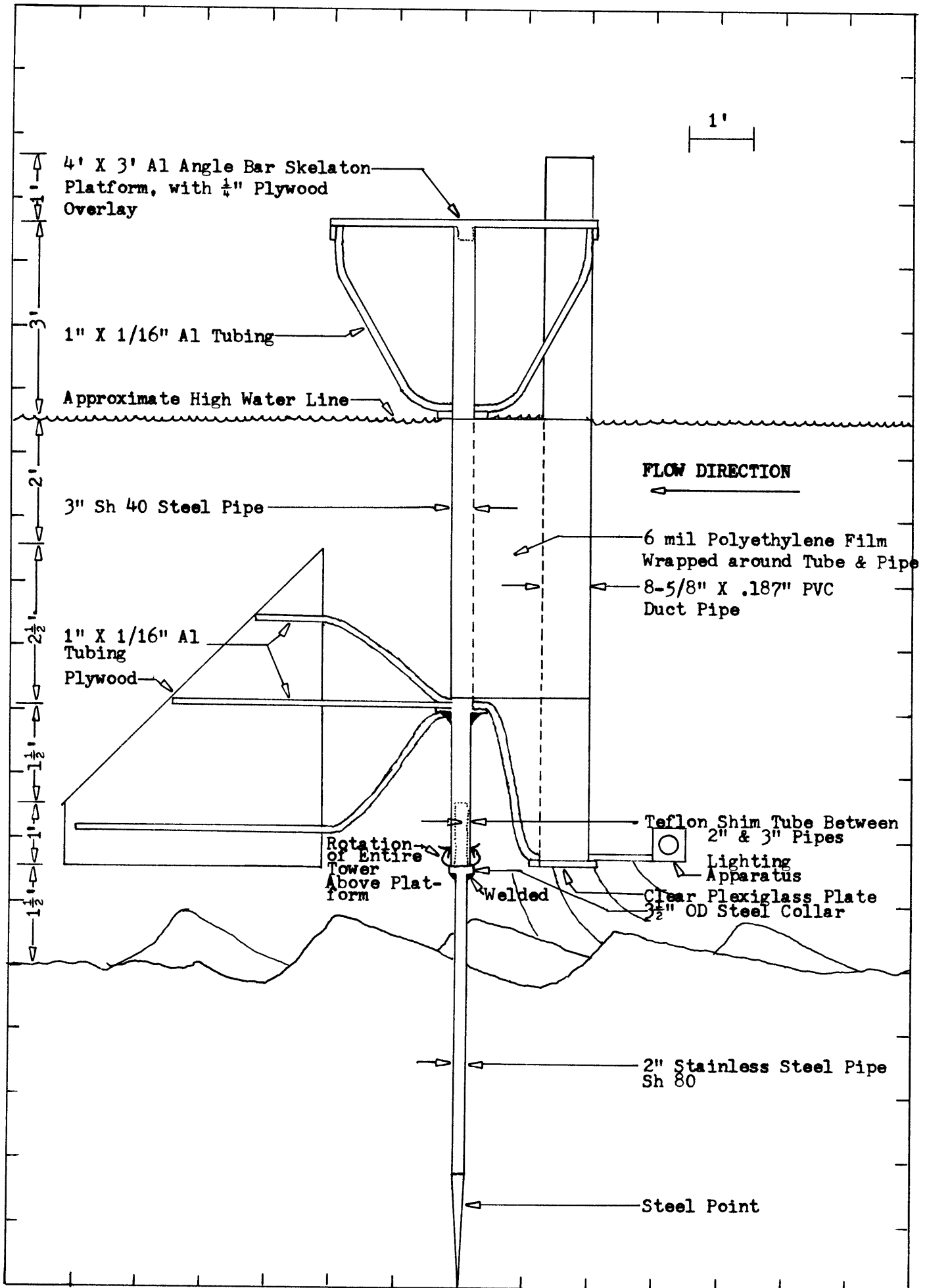
Various methods, yielding limited success, have been employed by previous investigators to determine migration rates of bed configurations in tidal environments. These methods will be critically examined in this section, and an alternative method will be proposed for the collection of more accurate and reliable data.

Hartwell (1969) discusses (among other things) the migration of a flood-oriented sand wave during a 45-day period. His method of measurement is to drive a series of marker-stakes at the slip-face of the sand wave, and then periodically record the distance of migration from the stakes. He found that the rates of migration were greatest during spring tides and least during neap tides. That is, his method is quantitative for tidal seasons, and as such, for determination of slow migration rates for extended periods of time, this method is fine. If, however, an attempt were made to extrapolate any information relating to the migration rate as a function of time within a tidal cycle from this general qualitative method, then this approach would be unacceptable. Knowledge of seasonal migration rates does not at all enable predictions of migration rates during tidal cycles. An attempt to apply this method to smaller bed forms with higher migration rates may not be legitimate. Certainly ripples, whose orientations can change within a tidal cycle, and perhaps dunes may migrate and change character at rates great enough to disallow for investigation by this method.

Klein (1970) and Klein and Whaley (1972) used dyed acrylic beads to determine a range of sediment dispersion and bedform migration over a tidal cycle. Again, this method does not give data for what happens during the tidal cycle. Klein and Whaley recognized the absence of this information and attempted to collect such data by observing the surface undulations (boils) and noting that the existence of a boil means that the bed form is migrating. On two "unusually calm days" the water surface was observed to display boils, and hence, they report sand wave and dune migration at particular periods of the tidal cycle. During these surface observations, bottom current velocities and depth were recorded to give velocity, depth, and bedform migration as a function of time over a tidal cycle. Not possible by this method are the actual rates of migration of the bed forms during the tidal cycle. Klein and Whaley also report that migration only begins after a sharp rise or fall in the bottom current velocity.

Examination of their data yields such skeptical information as: a dune 30 cm in amplitude submerged by more than 25 feet of water will produce a detectable surface boil. In addition, one questions the converse of their premise. Just because the presence of a surface boil implies bedform migration, the absence of a boil does not necessarily mean the absence of migration.

Hence, all previous methods of investigation have either failed to encompass the full scope of the problem or have fallen short of the goal. In the following pages, an apparatus and method is presented which will enable complete and accurate deter-



mination of the type of bedform, migration rates, and the nature of any transformations as functions of depth, velocity, and time during a tidal cycle.

Required for such a determination are methods for recording depth and velocity, recognizing bedforms, and measuring migration rates. On the page opposite is a plan view of the apparatus, basically conceived by John Southard, which is under final stages of construction and will enable all of the necessary determinations to be taken.

The main mast may serve as a tide guage, or an object may be lowered from the base of the platform to the surface of the water and subtracted from the height of the platform above the bed to give the depth of the water.

Due to the absence of a current meter, the following method is suggested for velocity measurement: an orange, which is nearly neutrally buoyant in seawater, is attached to a cord in which there is a knot tied at a known distance from the orange; while being timed, the orange which has been lowered to the water is allowed to drift freely until all of the cord up to the knot is let out. By trigonometry, the distance of travel of the orange is calculated, and the velocity may be determined by simple division. This velocity, it must be remembered, is the surface velocity. In laboratory experiments, the velocity is generally determined from an orifice meter, and hence, is a mean velocity. Therefore, for comparison of the data, a relationship is needed to relate surface velocity to mean velocity. This relationship

is derived and accompanied by a detailed description of its inherent limitations in Appendix 3.

The type of bedform, transformations, and migration rates will be determined by direct observation through a viewing tube, which extends from above the platform into the water to about $1\frac{1}{2}$ feet above the bed configurations. This viewing tube is about 8 inches in diameter and has a clear, plexiglass, water-proof window at its base. The bed will be illuminated by a lighting apparatus to one side of the viewing tube, permitting direct observation and photography of the bottom. In addition, a point gauge with a 2-inch square foot will be mounted, enabling bed profiles to be taken.

REFERENCES

- Allen, J.R.L., 1970, Physical Processes of Sedimentation, American Elsevier Publishing Company, Inc., New York. p. 76-78.
- American Society of Civil Engineers, Task Force on Bed Forms in Alluvial Channels, 1966b, Nomenclature for bed forms in alluvial channels: Am. Soc. Civil Engineers Proc., Jour. Hydraulics Div., v. 92, no. HY3, p. 51-64.
- Boothroyd, J.C., 1969 Essex Bay sand bodies; a preliminary report: in Coastal Environments, Field Trip Eastern Section Soc. Econ. Paleontologists and Mineralogists. p. 127-144.
- Boothroyd, J.C., 1969, Hydraulic conditions controlling the formation of estuarine bedforms: in Coastal Environments, Field Trip Eastern Section Soc. Econ. Paleontologists and Mineralogists. p. 417-427.
- Bruun, P., 1966, Tidal Inlets and Littoral Drift. American Society of Civil Engineers: Coastal Engineering Special Conference, Santa Barbara, California, October, 1965; and Hydraulics Division Conference, Madison, Wisconsin, August 1966. 193 p. Published as vol. 2 of Bruun, P., and Gerritsen, F., 1960, Stability of Coastal Inlets.
- Bruun, P., and Gerritsen, F., 1960, Stability of Coastal Inlets. North-Holland Publishing Company, Amsterdam. 123 p.
- Coleman, J.M., 1969, Brahmaputra river: channel processes and sedimentation: Sediment. Geology, v. 3, p. 129-239.
- Daley, J.W., and Harleman, D.R.F., 1966, Fluid Dynamics. Addison-Wesley Publishing Company, Inc., Reading, Mass. 454 p.
- Folk, R.L., 1965, Petrology of Sedimentary Rocks. University of Texas, Austin. p. 34-64.
- Guy, H.P., Simons, D.B., and Richardson, E.V., 1966, Summary of alluvial channel data from flume experiments, 1956-1961: U.S. Geol. Surv. Prof. Paper 462-I, 96 p.
- Hartwell, A.D., 1969, Tidal Delta, Merrimack River Estuary: in Coastal Environments, Field Trip Eastern Section Soc. Econ. Paleontologists and Mineralogists. p. 184-203.
- Kennedy, J.F., 1963, The mechanics of dunes and antidunes in erodible-bed channels: Jour. Fluid Mech., v. 16, p. 521-544.

- Keulegan, G.H., 1967, Tidal flows in entrances: water-level fluctuations of basins in communication with seas: U.S. Army Corps of Engineers, Committee on Tidal Hydraulics Technical Bulletin No. 14.
- Klein, G.deV., 1970, Depositional and dispersal dynamics of intertidal sand bars: Jour. Sed. Petrology, v. 40, p. 1095-1127.
- Klein, G.deV., and Whaley, M.L., 1972, Hydraulic parameters controlling bedform migration on an intertidal sand body: Geol. Soc. America Bull., v. 83, p. 3465-3470.
- Simons, D.B., and Richardson, E.V., 1963, Forms of bed roughness in alluvial channels: Am. Soc. Civil Engineers Trans., v. 128, part I, p. 284-302.
- Simons, D.B., Richardson, E.V., and Nordin, C.F., Jr., 1965, Sedimentary structures generated by flow in alluvial channels: Soc. Econ. Paleontologists and Mineralogists, Spec. Pub. 12, p. 34-52.
- Smith, N.D., 1971, Transverse bars and braiding in the Lower Platte River, Nebraska: Geol. Soc. America Bull., v. 82, p. 3407-3420.
- Southard, J.B., 1971, Representation of bed configurations in depth-velocity-size diagrams: Jour. Sed. Petrology, v. 41, p. 903-915.
- Strahler, A.N., 1966, A Geologist's View of Cape Cod. The Natural History Press, Garden City, New York. 115 p.
- Tide Tables, High and Low Water Predictions, 1973, East Coast of North and South America Including Greenland, U.S. Department of Commerce.
- Yalin, M.S., 1964, Geometrical properties of sand waves: Am. Soc. Civil Engineers Proc., Jour. Hydraulics Div., v. 90, no. HY5, p. 105-119.

APPENDIX 1

Sieve Analyses

Sieve Analyses were done on two sands collected at Nauset Inlet. The linear dune sand was obtained at the location observed in photo #4, page 21, and the fully developed dune sand is from the proposed study location shown in photo #3, page 20. Both sands are moderately to very well sorted by the classification set forth by Folk (1965). The fully developed dune sand has a slightly coarser median grain size than the linear dune sand, which is to be expected since fully developed dunes are in a higher flow regime.

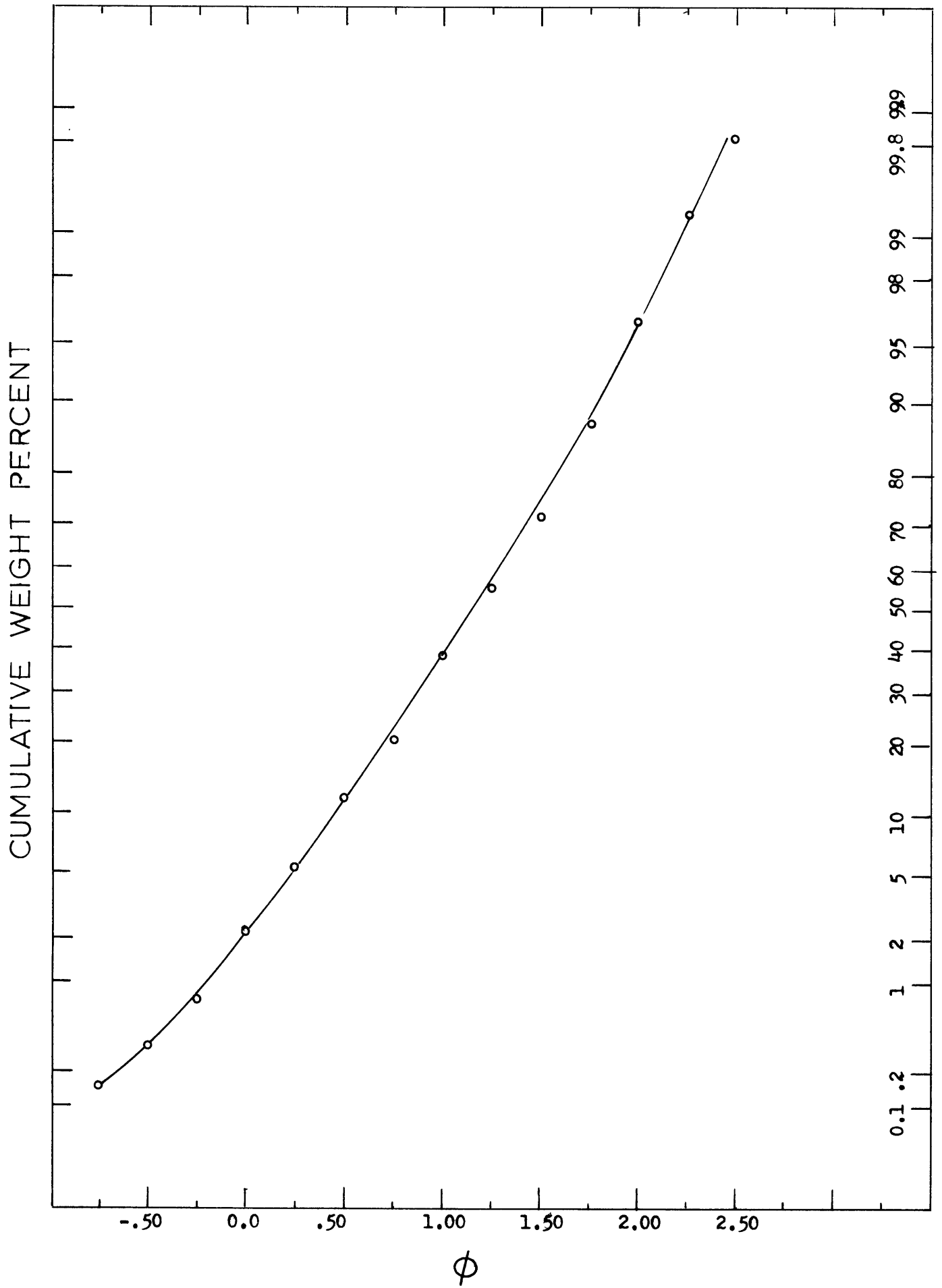
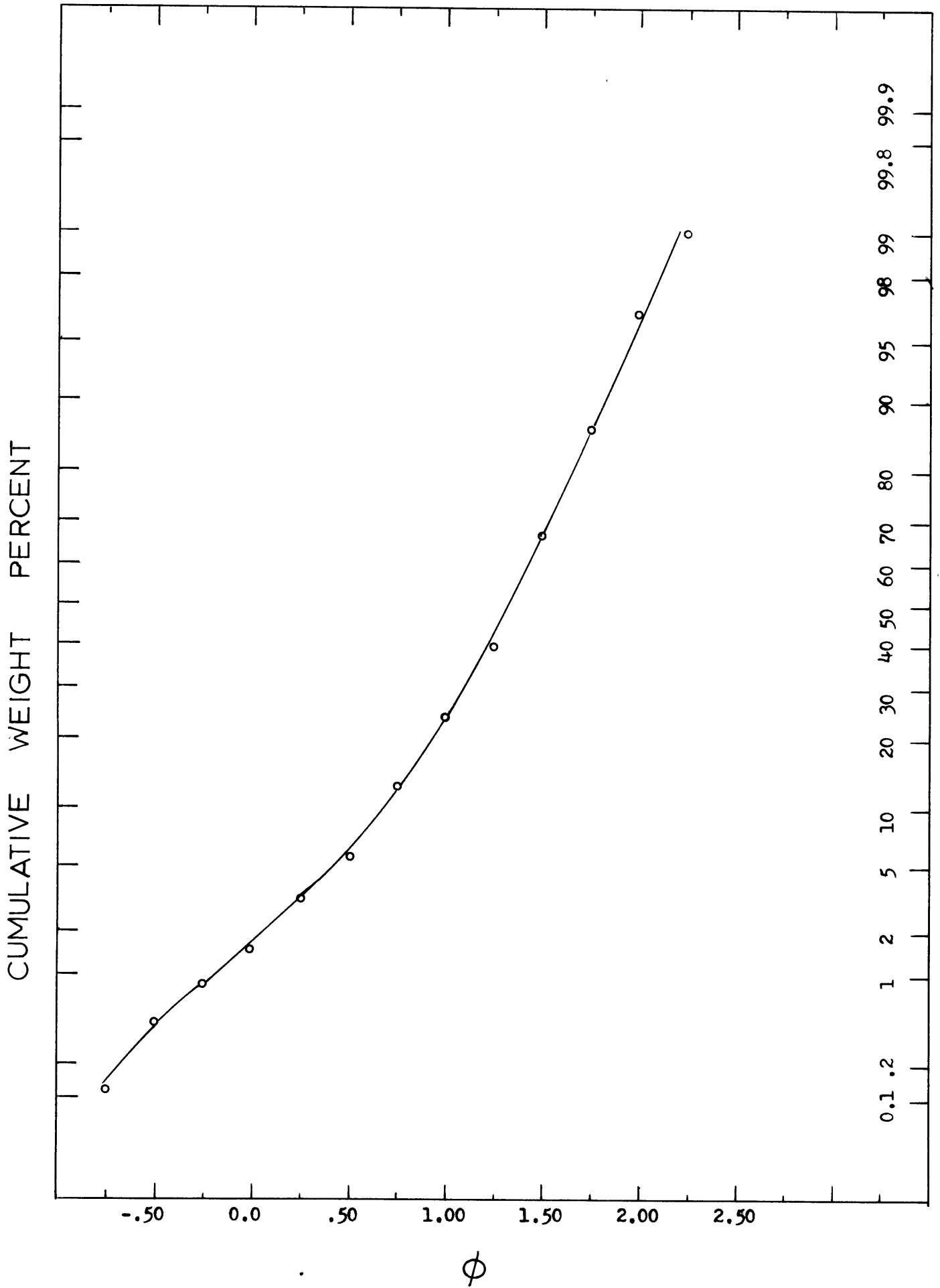


Figure 6

FULLY DEVELOPED DUNES



APPENDIX 2

Photographs of Bed Configurations
Observed in Similar Environments

The following collection of photographs are of bed configurations which were observed when aerial reconnaissance photography was undertaken to determine the most probable study location. Selected from among some fifty photographs, these seven are particularly helpful in qualitatively understanding the nature of bedforms in tidal environments. Not only are bedforms observed which are similar to those in Nauset Inlet, but other bed configurations--obviously as a result of slightly different hydrodynamic conditions--are also shown.

It is to be noted that the nomenclature used in identification of the bedforms is based solely on the aerial photography, since no field observations of these environments were taken. As such, further investigation of these features may prove that some of the nomenclature is incorrect.



Figure 1. Aerial photograph of an intertidal sand bar in Barnstable Harbor channel. Note development of a dune field along the sand bar. Lower left corner of photo shows more fully developed dunes with larger amplitudes than upper right corner where there are more linear dunes. There is also a lateral decrease in dune development from left to right across the sand bar. Both effects are the result of decreasing depth and velocity across and around the sand bar. The direction of flood flow is diagonally from left to right, implying that the dunes are flood oriented. Smith (1971) has observed that fully developed dunes form in the deeper and upstream portions of the sand bar for alluvial flow conditions. The two observations, then, are compatible. Photo taken about two hours after low tide for Barnstable Harbor during late afternoon looking west.



Figure 2. Aerial photograph of a Great Salt Marsh meandering tidal channel near Barnstable. Note development of more or less linear dunes in channel bottom, presumably due to an elevation difference caused by a meandering thalweg. Sand body in upper right corner of photo due to sub-aerial deposition from a beach source off the right of the photograph. Photo taken about two hours after low tide for Barnstable Harbor.

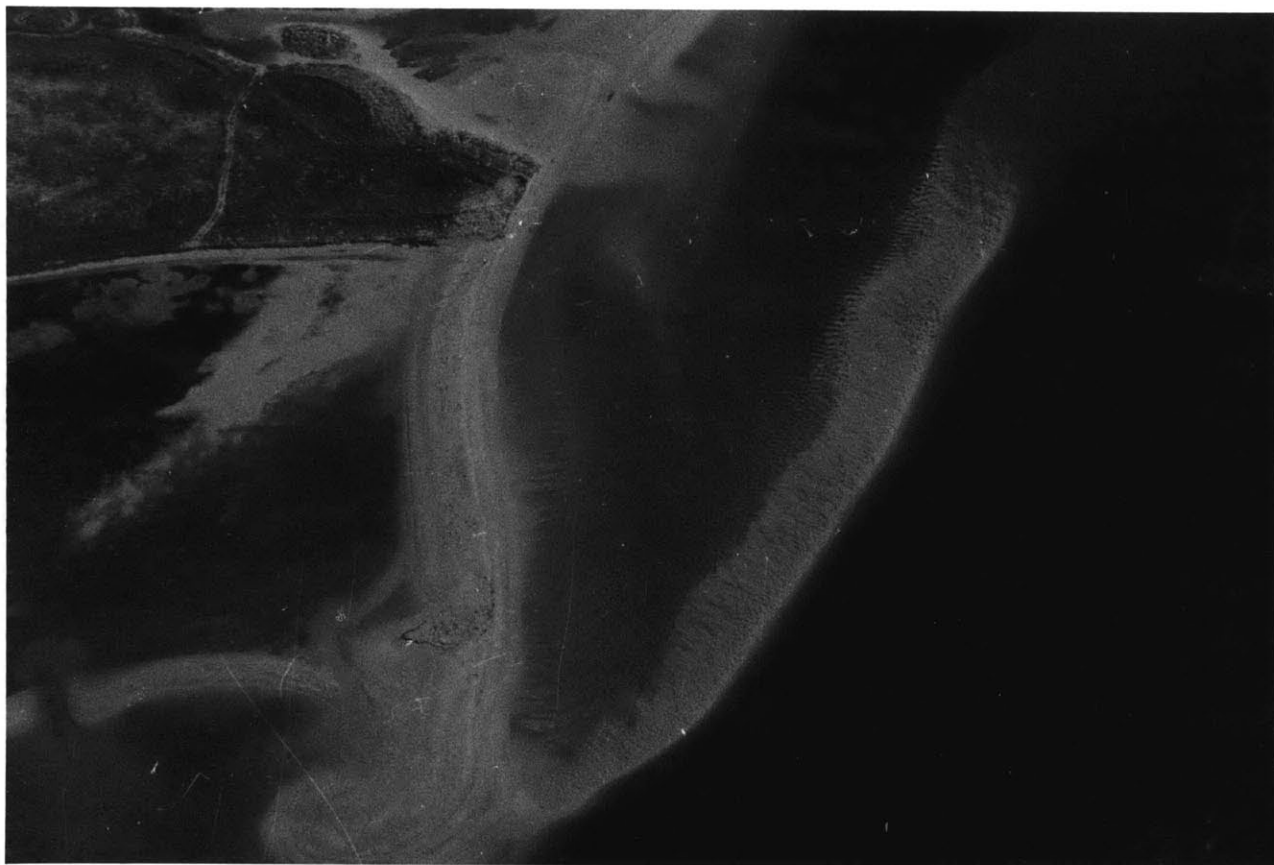


Figure 3. Vertical aerial photograph of subtidal and intertidal dunes along one side of a sand bar at mouth of Chatham Harbor. Atlantic Ocean is on right, and harbor entrance off picture on bottom. Apparent dune amplitudes appear to be in agreement with Smith's observations as discussed in Figure 1. Note also linear features on inside of main sand body. Presumably these are migrating toward the main harbor entrance. Note also erosion of coastline in upper portion of photo. Photo taken about one hour after low tide for the harbor entrance.

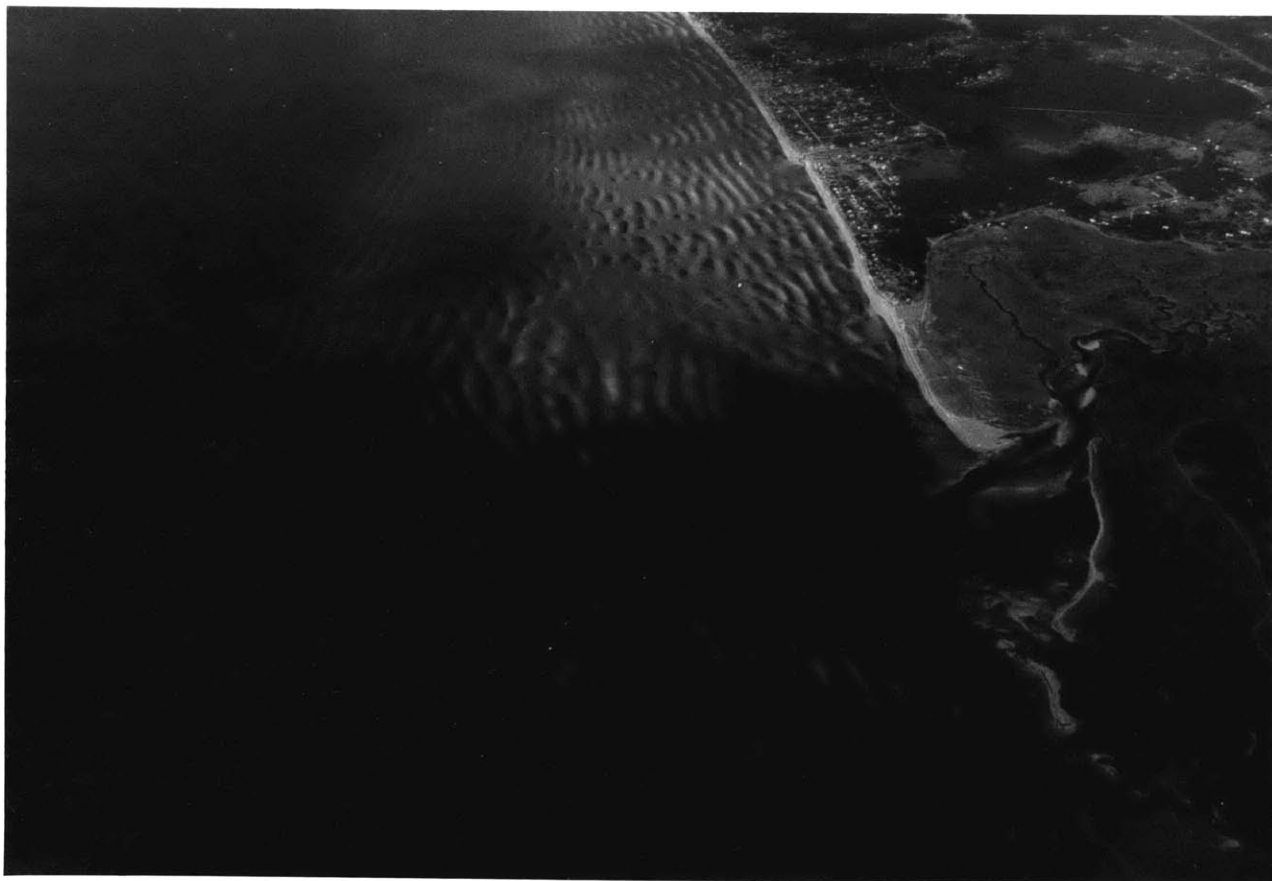


Figure 4. Aerial photograph overlooking the bay side of Cape Cod facing northeast. Readily apparent are large, linear, intertidal and subtidal sand ridges exhibiting approximately equal spacing. The amplitudes appear to show a slight increase landward. Note disruption and absence of features due to off-shore drainage and tidal channels. Main tidal channel is located near First Encounter Beach, and dune formation has been observed there by John Southard. Note also the occurrence of three or four sand bars alternating sides along the tidal channel. Atlantic coast visible in upper right corner of photo. Photo taken at low tide.

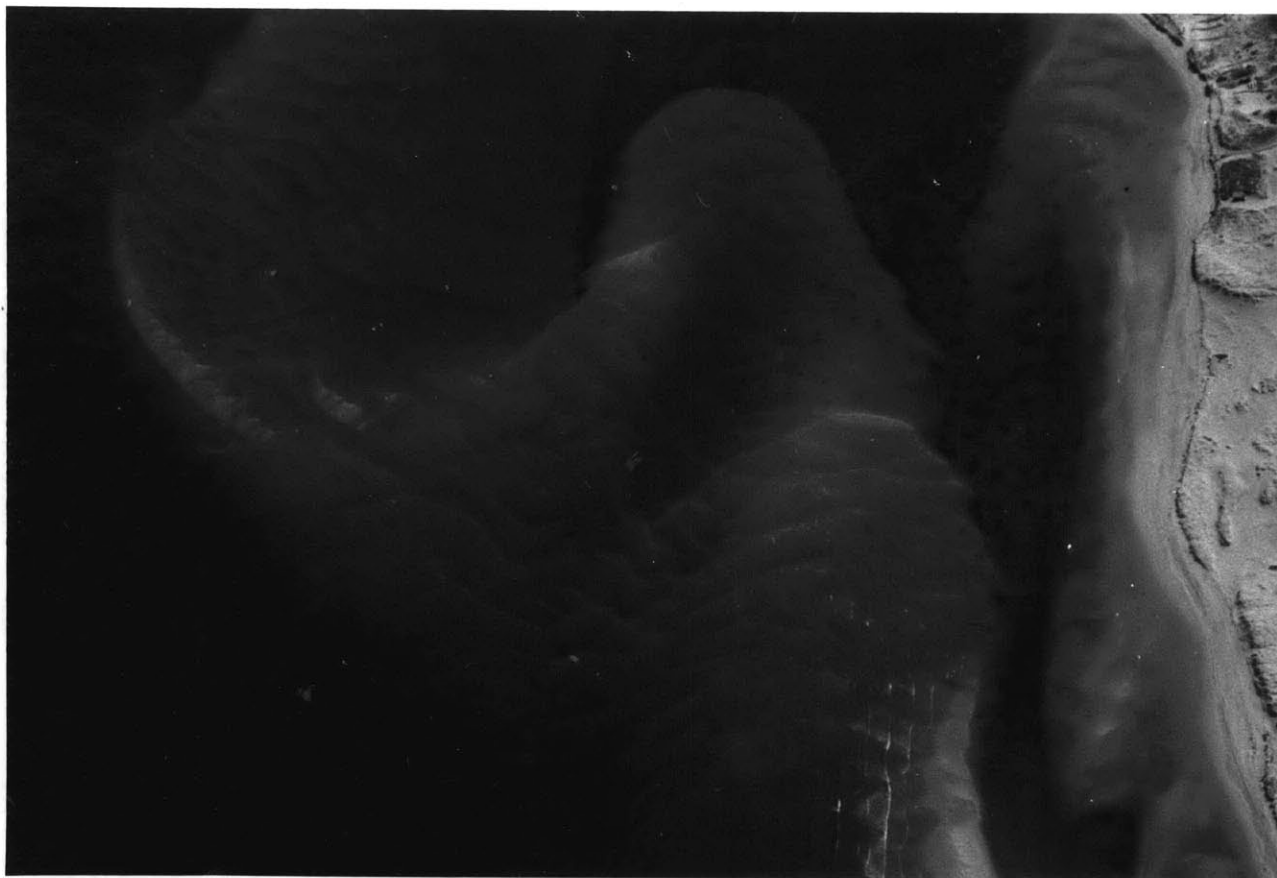


Figure 5. Vertical aerial photograph taken about an hour after low tide in Chatham Harbor channel. Note development of sub-tidal-intertidal sand bars and sandwaves. The sand bars can be seen breaking surface in several places. Note also the linear arrangement of crests parallel to the shore in the lower right portion of the photograph. The nature of these crests is strikingly similar to the features observed in figure 4. The striations in the lower central portion of the picture are surface waves caused by a motor boat.

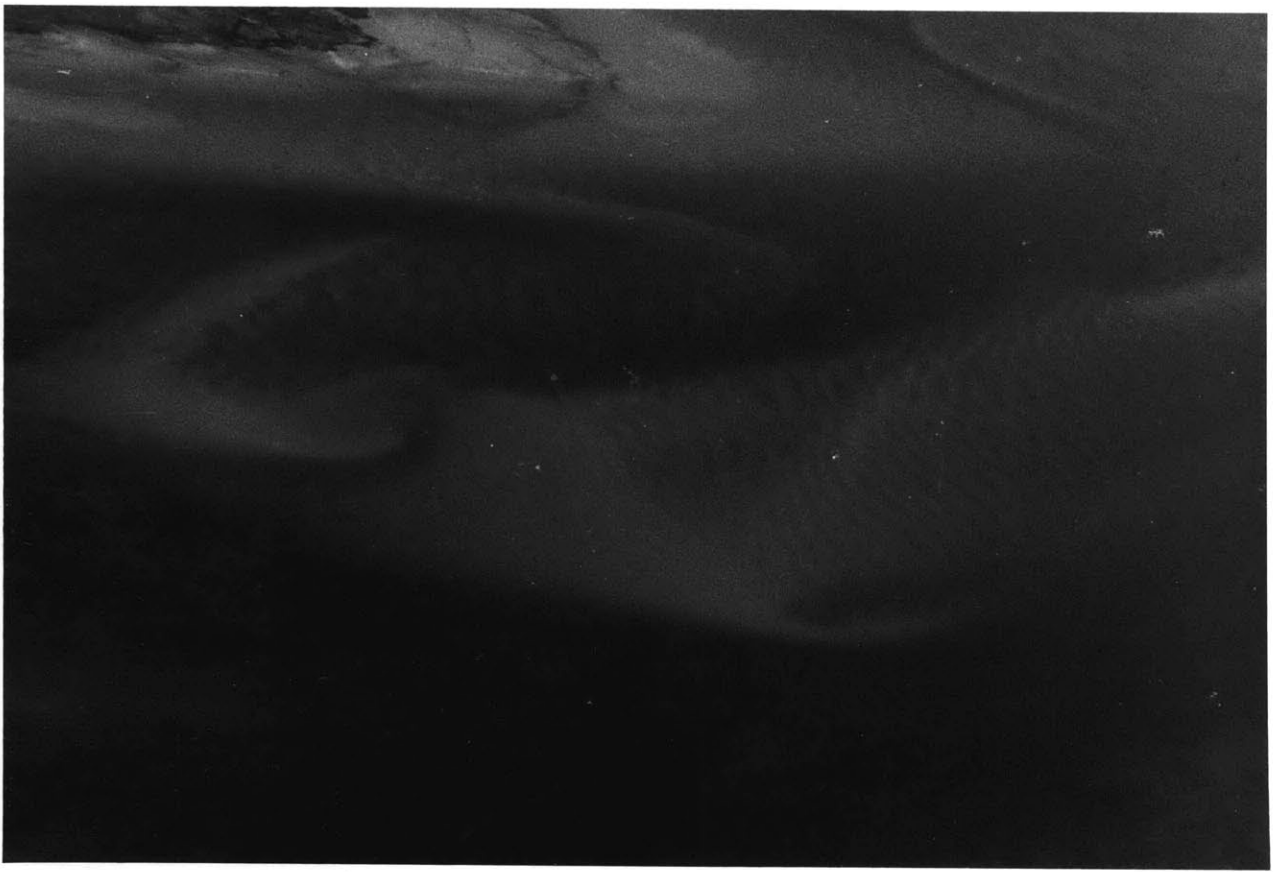


Figure 6. Aerial photograph of subtidal sand waves and sand bars several miles landward in Chatham Harbor channel. Photo taken about an hour after low tide, looking east near location of figure 5.



Figure 7. Aerial photograph of subtidal interference sand waves farther landward in Chatham Harbor channel than figures 5 and 6. Photo taken about an hour after low tide.

APPENDIX 3

Relation Between Mean Surface Velocity
and Mean Velocity

The following section contains the derivation between mean surface velocity and mean velocity of the entire flow for two-dimensional, infinitely wide, steady, uniform, open channel flow and includes a discussion about the nature of the assumptions involved and their physical limitations.

Due to the nature of the experiment, surface velocity measurements are readily accessible, whereas in laboratory studies a mean velocity for the flow is determined. Hence, in order to correlate the data obtained in the field with those from laboratory experiments, a relation is needed between the surface velocity and the mean velocity for field conditions. From Daley and Harleman, (1966) the velocity-defect law for two-dimensional flow in an open channel whose width is many times its depth may be given as

$$\frac{\bar{U} - \bar{u}}{u_*} = \frac{-2.3}{K} \log \frac{y}{y_0}, \quad (1)$$

where \bar{U} = undisturbed mean surface velocity

\bar{u} = mean velocity of the entire flow

u_* = shear velocity

y = elevation to the point which has a velocity = \bar{u}

y_0 = depth of the flow

K = von Karman's constant.

The mean velocity may be approximated as the velocity which occurs at $\frac{y}{y_0} = 0.6$. Also, if von Karman's constant is assigned the value of 0.4, the velocity-defect law may be rewritten as

$$\bar{U} - \bar{u} = 1.28u_* \quad (2)$$

Now
$$u_* = \sqrt{\tau_0 / \rho} = \sqrt{g R_h S_0} \quad (3)$$

where R_h = hydraulic radius = $\frac{\text{flow cross section}}{\text{wetted perimeter}}$.

For a rectangular channel of depth D and width W , the flow cross section = DW , and the wetted perimeter = $2D + W$. For an infinitely wide channel, the hydraulic radius may be written as

$$\lim_{W \rightarrow \infty} R_h = \frac{DW}{2D+W} \quad (4)$$

Factoring out a W from both the numerator and the denominator, and noting that $\frac{2D}{W} \rightarrow 0$ as $W \rightarrow \infty$, gives

$$\lim_{W \rightarrow \infty} R_h = \frac{W}{W} \left[\frac{D}{\frac{2D}{W} + 1} \right] = D \quad (5)$$

Hence, for an infinitely wide channel with a finite depth, the hydraulic radius is merely equal to the depth.

Now the shear velocity may be written as a function of the friction factor:

$$u_* = \bar{U} \sqrt{f/8} \quad (6)$$

and, by substituting this expression for the shear velocity in the velocity-defect law, equation (2), and solving for \bar{U} gives,

$$\bar{U} = \bar{u} \left[\frac{1}{1 - 1.28 \sqrt{f/8}} \right] \quad (7)$$

This may be expressed as

$$\bar{U} = \bar{u} \left[\frac{1}{1 - x} \right], \quad \text{where } x = 1.28 \sqrt{f/8} \quad (8)$$

By Taylor expansion,

$$\bar{U} = \bar{u} (1 + x + x^2 + \dots + x^n), \quad (9)$$

and hence, for small x this reduces to

$$\bar{U} = \bar{u} (1 + x), \quad \text{or} \quad (10)$$

$$\bar{U} = \bar{u} (1 + 1.28 \sqrt{f/8}). \quad (11)$$

This equation relates the surface velocity to the mean velocity times a correction factor which arises from the bottom friction. With increasing depth, these bottom viscous effects become less significant to the outer region of the velocity profile, and the mean velocity of the flow should approach that of the surface. That is, as the correction factor goes to zero, \bar{u} goes to \bar{U} , which is immediately evident from the equation.

As the depth decreases the flow conditions are dominated by wave action and swash zone activity - conditions of high non-uniformity and unsteady flow, and the velocity profile is also affected by bottom viscous effects and suspended sediment. As a result, the correction factor is not small and this relation cannot be applied during these water conditions. For depths greater than about 1 1/2 feet, this relation begins to become meaningful.

The problem of determining what value to assign to the friction factor, f , has been investigated by many authors. It is generally considered that f is a function of the sand grain roughness, in addition to correlating in some complicated way to the geometrical properties of the bedforms. Simons and Richardson (1961) investigated the variation of the friction factor as a function of grain size and bedform. For the .28mm sand, f varied from .0635 to .1025 for ripples, and from .0612 to .0791 for dunes. For the .45mm sand, f varied from .054 to .1330 for ripples, and from .0489 to .1490 for dunes. Also the actual effect of the degree of sorting of the sand on the friction factor is not understood, but is

obviously more important in field conditions than in prepared sands used in the laboratory Bruun (1966) notes that the friction factor is greater for uniform sands than graded sands. The sands in the study area lie about midway between these two degrees of sorting, and hence, only moderate values of the friction factor would be expected at the study area. In addition, the friction factor appears to be dominated by very local conditions, and hence, for ripples superimposed on dunes, the ripples tend to be the dominating factor in determining the friction factor. Finally, since in the determination of the mean velocity, the friction factor appears as $1.28\sqrt{f/8}$, a large variance in the value of f yields only a very small variance for the entire correction factor. For all of these reasons, one may choose $f = .08$, giving

$$\bar{U} = 1.128\bar{u} . \quad (12)$$